communications biology

A Nature Portfolio journal

Article

https://doi.org/10.1038/s42003-025-08191-9

DNAJC5 facilitates the proliferation and migration of lung adenocarcinoma cells by augmenting EGFR trafficking

Can Chen[1,2], Linlin Xu[3], Limin Chen[1], Zhenyu Zhai[1], Minzhang Cheng[4], Shiwen Luo[2] ✉ & Hailong Wang[1] ✉

Lung adenocarcinoma (LUAD) is a highly prevalent and lethal malignant tumor, with the aberrantly activated EGFR signaling pathway playing a crucial role in its development. However, resistance to tyrosine-kinase inhibitors (TKIs) targeting EGFR significantly limits the efficacy of LUAD clinical therapy. Therefore, it is imperative to identify novel therapeutic targets and elucidate the regulatory mechanisms of EGFR for improving LUAD treatment outcomes. In this study, we discover that DNAJC5 functions as an oncogene in LUAD. We observe elevated protein levels of DNAJC5 in tissues from LUAD patients, which are strongly associated with poor prognosis among these individuals. Furthermore, overexpression of DNAJC5 promotes proliferation and migration of LUAD cells both in vitro and in vivo. Mechanistic investigations reveal that DNAJC5 interacts with the intracellular domain of EGFR and enhances its endocytosis and recycle, thereby augmenting EGFR activity and downstream signaling pathways. Additionally, we find that DNAJC5 binds to AP2A1 protein—a key player in EGFR endocytosis—and strengthens its interaction with EGFR. Knockdown experiments targeting AP2A1 attenuate the ability of DNAJC5 to promote proliferation and migration of LUAD cells. Collectively, our findings unveil a functional role for DNAJC5 in regulating EGFR trafficking and driving LUAD progression.

Lung cancer is one of the most prevalent malignancies worldwide, exhibiting high incidence and mortality rates, resulting in approximately 1.76 million deaths annually[1]. Histopathologically, lung cancer can be broadly classified into four categories: lung adenocarcinoma, lung squamous cell carcinoma, large cell lung cancer, and small cell lung cancer. Among these subtypes, lung adenocarcinoma accounts for approximately 50% of all cases[2]. Despite significant advancements in targeted therapy and immunotherapy, these two approaches only target a specific subset of patients with lung adenocarcinoma, and the overall survival rate remains alarmingly low.

Epidermal growth factor receptor (EGFR), a member of the ErbB/HER family of receptor tyrosine kinases (RTKs), plays a critical role in regulating epithelial cell growth, metastasis, and invasion. It serves as a prominent therapeutic target for treating lung adenocarcinoma[3]. The first- and second-generation EGFR tyrosine kinase inhibitors (TKIs) such as erlotinib, gefitinib, afatinib, and dacomitinib have been extensively utilized to treat patients with Wild-type EGFR (WT-EGFR) or those harboring EGFR-activating mutations (exon 19 deletions and L858R mutation). These TKIs have shown remarkable efficacy. However, a substantial proportion of patients with lung adenocarcinoma develop resistance to EGFR-TKIs. Among them about 50% exhibit resistance due to the presence of an EGFR T790M mutation[4]. Third-generation EGFR TKIs like rociletinib and AZD9291 have been developed specifically to overcome TKI resistance mediated by the EGFR T790M mutation. Unfortunately, newly acquired resistant mutations including EGFR C797S and EGFL718Q have also been reported in some patients[5]. Thus, there is an urgent need to explore novel mechanisms involved in EGFR signaling activation which is vital for finding new targets and improving therapeutic efficacy.

As a receptor, EGFR is predominantly localized on the cell surface. Upon stimulation by ligands such as EGF, EGFR forms dimers and

[1]Medical Innovation Center, The First Affiliated Hospital, Jiangxi Medical College, Nanchang University, Nanchang, Jiangxi, China. [2]Center for Experimental Medicine, The First Affiliated Hospital, Jiangxi Medical College, Nanchang University, Nanchang, Jiangxi, China. [3]Department of Pathology, The First Affiliated Hospital, Jiangxi Medical College, Nanchang University, Nanchang, Jiangxi, China. [4]Jiangxi Institute of Respiratory Disease, the Department of Respiratory and Critical Care Medicine, The First Affiliated Hospital, Jiangxi Medical College, Nanchang University, Nanchang, Jiangxi, China. ✉e-mail: shiwenluo@ncu.edu.cn; ndyfy05389@ncu.edu.cn

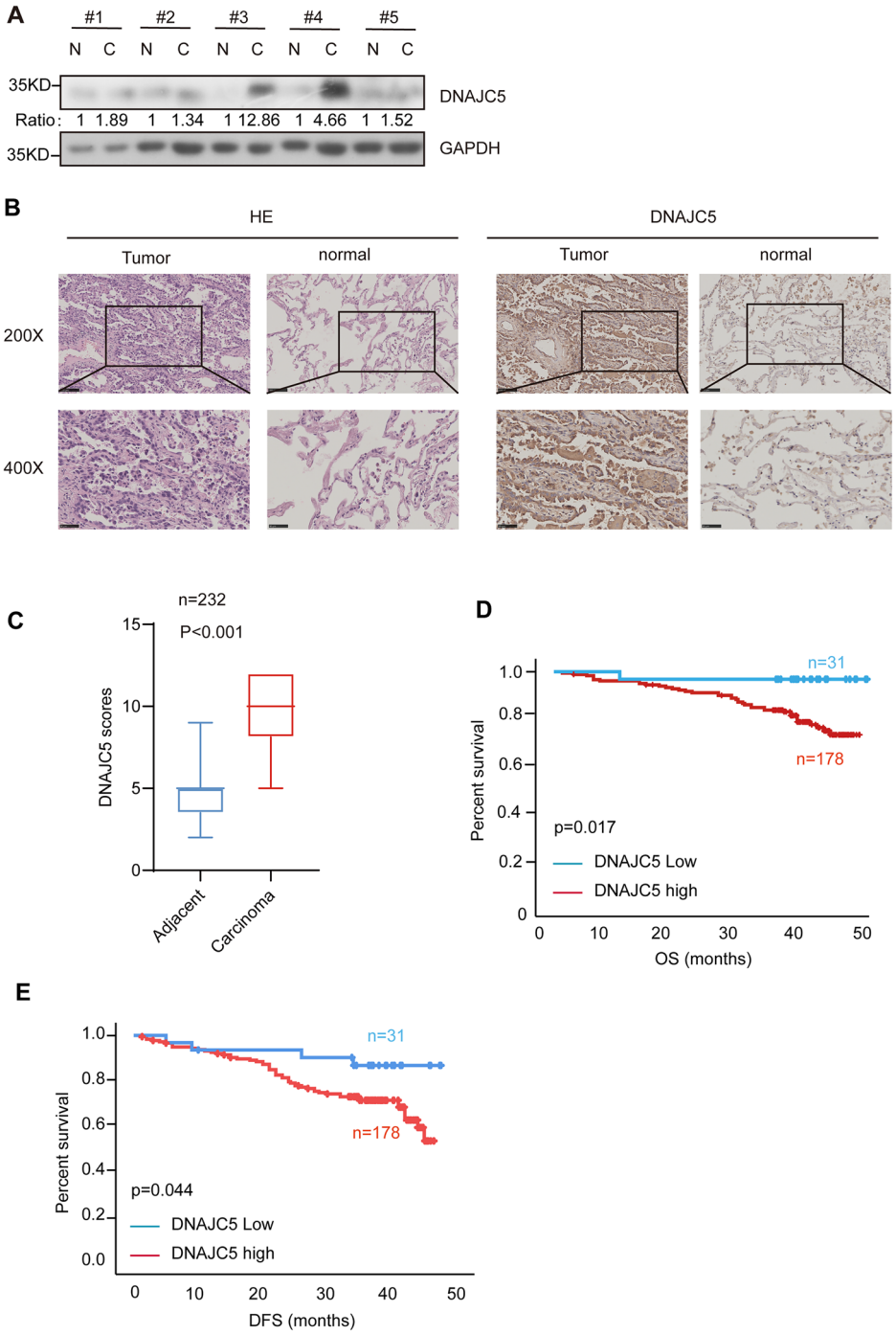

Fig. 1 | DNAJC5 exhibits high expression levels in lung adenocarcinoma tissues. A Western blot analysis was performed to detect the protein expression levels of DNAJC5 in five randomly selected pairs of LUAD and matched adjacent tissues. N represents normal tissue; C represents tumor tissue. **B** Immunohistochemical staining was conducted to visualize the expression of DNAJC5 in representative LUAD and adjacent tissues. **C** The expression levels of DNAJC5 were evaluated and scored in both LUAD and adjacent tissues. Plots illustrating the scores for DNAJC5 expression are presented. Statistical significance was determined using the Mann-Whitney U test with a sample size (*n*) of 232. **D**, **E** Kaplan-Meier survival rate analyses were performed to assess overall survival (**D**) and disease-free survival (**E**) rates among 209 LUAD patients stratified based on IHC-assessed DNAJC5 levels.

undergoes auto-phosphorylation, subsequently activating multiple signal transduction pathways[6]. Simultaneously, ligand-induced internalization of EGFR occurs through both clathrin-mediated endocytosis (CME) and various non-clathrin endocytosis (NCE) pathways depending on growth conditions and cellular context[7]. At low concentrations of EGF, CME primarily mediates the internalization of EGFR followed by recycling back to the plasma membrane; however, approximately 30% of receptors are targeted for degradation. Conversely, at high doses of EGF (20–100 ng/ml), NCE is activated leading to lysosomal degradation of EGFR which attenuates its signaling capacity[8]. Aberrant expression and dysregulated trafficking of EGFR result in mis-localization and enhanced downstream signaling activity, contributing to cancer development[9]. Clathrin-mediated endocytosis has been reported to contribute to primary resistance against gefitinib treatment in wild-type EGFR NSCLC[10]. Similarly, inhibition of EGFR endocytosis reduces cell viability and promotes apoptotic cell death in vitro and in vivo models of gefitinib-insensitive lung cancer harboring wtEGFR mutations[11]. Therefore, elucidating the mechanisms underlying EGFR trafficking holds promise for identifying potential therapeutic targets for cancers driven by aberrant activation of EGFR.

DNAJC5, also known as Cysteine string protein α (CSPα), is a member of the DnaJ/Hsp40 family of co-chaperones[12]. The protein contains three functional domains. The conserved N-terminal J-domain binds heat shock protein 70 (HSP70) and activates its ATPase activity, assisting HSP70 in refolding or degrading target proteins. The cysteine-enriched "cys-string domain" (cys), heavily palmitoylated, regulates DNAJC5's membrane association and trafficking. Another domain connecting the J domain and the cys domain is a "linker domain"[13]. Although DNAJC5 is widely detected in all tissues, it is predominantly enriched in neurons where it plays a crucial

Table 1 | Association of DNAJC5 expression levels with clinicopathologic characteristics in LUAD

Clinicopathologic characteristics	*n*	DNAJC5 expression		*p*-value
		High (%)	Low (%)	
Gender	210			
Male		87 (41.4%)	14 (6.7%)	0.702
Female		91 (43.3%)	17 (8.1%)	
Age (years)	210			
< 60		88 (42.1%)	17 (8.1%)	0.579
≥ 60		90 (43.1%)	14 (6.7%)	
Tumor size (cm)	210			
≤ 3		114 (54.5%)	18 (8.6%)	0.524
> 3		64 (30.6%)	13 (6.2%)	
Differentiation	210			
Well		53 (25.2%)	14 (6.7%)	**0.007**
Moderate		71 (33.8%)	11(5.2%)	
Poor		54 (25.7%)	6 (2.9%)	
Lymph node metastasis	210			
Yes		61 (29.2%)	9 (4.3%)	0.569
No		117 (56.0%)	22 (10.5%)	
TNM stage	210			
StageI-II		163 (78%)	26 (12.4%)	0.188
StageIII-IV		15 (7.2%)	5 (2.4%)	
Metastasis	210			
Yes		55 (26.3%)	3 (1.4%)	**0.015**
No		123 (58.9%)	28 (13.4%)	
Smoke	210			
Yes		69 (33.3%)	12 (5.8%)	0.958
No		107 (51.7%)	19 (9.2%)	

Association of DNAJC5 expression levels with clinicopathologic characteristics in LUAD. Statistically significant $p < 0.05$ values are in bold.

role in maintaining synaptic homeostasis[14]. Mutation or knockout of DNAJC5 in Drosophila, worms and mice causes synaptic dysfunction, neurodegenerative changes and premature death[15]. Additionally, DNAJC5 mutations are closely associated with several human diseases such as Neuronal ceroid lipofuscinosis, Huntington's disease, cystic fibrosis, and Parkinson's disease[16–18]. However, little has been discussed about the function of DNAJC5 in cancer. We initially discovered that DNAJC5 acts as an oncogene in hepatocellular carcinoma by promoting cell proliferation through regulating SKP2-mediated p27 degradation[19]. Subsequently, we investigated whether DNAJC5 was involved in other cancer progressions. Through analysis of clinical tumor tissues and adjacent tissues from LUAD patients, we found that DNAJC5 expression was significantly higher in LUAD tissues compared to adjacent tissues, and high levels of DNAJC5 expression were positively correlated with poor prognosis for LUAD patients. Therefore, in this study we aim to explore the role of DNAJC5 in LUAD progression along with its underlying molecular mechanism.

Materials and methods

Cell lines

A549, HEK293T and NCI-H1299 were cultured in Dulbecco's modified minimal essential medium (Gibco; C11995500BT) and BASIC RPMI 1640 Medium (C11875500BT) respectively, supplemented with 10% FBS (Excell; FSP500), 1% penicillin/streptomycin (Gibco; 15140-122) in a humidified atmosphere at 37 °C with 5% CO_2. All cells were purchased from the American Type Culture Collection (ATCC, Manassas, VA).

The DNAJC5-overexprssion A549 cell lines and DNAJC5 knock-down NCI-H1299 cell lines were constructed using lentivirus or retrovirus systems as described previously[19]. The effects were proved by western blot. The short hairpin (sh) RNA sequences were as following: shDNAJC5#1 (5'-GAAGCTTGCCTTGAAATAT-3'), shDNAJC5#2 (5'-AAGTCCTATCG-GAAGCTTG-3'), and shNon-Target (shNT) (5'-TTCTCCGAACGTGT-CACGT-3').

Plasmids and regents

The cDNAs of DNAJC5 and EGFR derived from HEK293T cells were cloned into mammalian expression vectors PcDNA3.1-Flag (Clontech) or pKH3-HA (Clontech). The plasmids for AP2A1, AP2M1, and AP2S1 were purchased from Miaoling biology company.

Transfection

HEK293T cells were seeded in 6-well plates for 24 h and transfected with the indicated plasmids by using Lipofectamine 2000 (Invitrogen) in accordance with the manufacturer's instructions. 48 h after transfection, the cells were harvested and subjected to co-immunoprecipitation and western blot.

Quantitative RT-PCR

The RNA from the indicated cells was extracted using TransZol Up kits (TransGen Biotech, China) and was utilized to synthesize the first-strand cDNA through the PrimeScript RT Reagent Kit (Takara Bio, Otsu, Japan) in accordance with the manufacturer's instructions. The mRNA levels of DNAJC5 were detected by Quantitative real-time PCR employing a SYBR Premix Ex Taq RT-PCR Kit (Takara Bio, Japan; RR820A) and analyzed using a CFX96 real-time PCR detection system (Bio-Rad). The relative expression levels of DNAJC5 were determined by normalization to GAPDH RNA levels. The primers were used as follows: GAPDH forward, 5′-CCACTCCTCCACCTTTGAC-3′; reverse, 5′-CCACTCCTCCACCTTT-GAC-3′; DNAJC5 forward, 5′- GGGAGTCATTGTAC-
CACGTCC-3′; reverse, 5′- CGTGCGCGTTGTTGATCTC-3′.

Western blotting and co-immunoprecipitation

Protein extracts were obtained using TNE buffers (50 mM Tris-HCl, 150 mM NaCl, 0.5% NP40, 1 mM EDTA, proteases inhibitors (sigma), PH 7.5) and subjected to western blot as described previously[19]. The immunoblot films were digitalized using an Epson V700 scanner, and the intensity of major bands was quantitated using Image J (National Institutes of Health, Bethesda, MD, USA). The primary antibodies were used as bellow: EGFR (CST, 4267), p-EGFR (CST, #3777), AKT (CST, #4691S), ERK (CST, #4695), p-AKT (CST, #4060S), p-ERK (CST, #4695), GFP (Sigma, G1544), DNAJC5 (Millipore, AB1576), Flag (Sigma, F3165), GAPDH (Millipore, MAB374), HA (CST, 3724S).

For co-immunoprecipitation (co-IP), the cells were transfected with indicated plasmids, washed with ice-cold PBS and lysed with TNE buffers. The cell lysates were then centrifugated at 13,000 g for 10 min at 4 °C and the supernatants were acquired. Subsequently, 1 μg of primary antibodies was incubated with the supernatants overnight at 4 °C followed by addition of protein A + G agarose beads (MCE, HY-K0202) for another three hours incubation at 4 °C. The beads were washed three times with lysis buffer(1 mL each time), boiled in SDS loading buffer for five minutes. Finally, the samples underwent western blot analysis as described above.

Mass Spectrometry (MS)

Whole cell lysates from HEK293T transfected with plasmids expressing DNAJC5-Flag were immunoprecipitated with anti-Flag magnetic Beads (HY-K0207, MCE) overnight. The beads were washed three times with PBS, and most of the beads were sent to Shangbai bioprofile company for LC-MS/MS sequencing and data analysis. A small amount of the remaining beads was eluted by SDS loading buffer, and the collected protein complex was separated on SDS-PAGE gel followed by silver staining (G2080-25T, Servicebio).

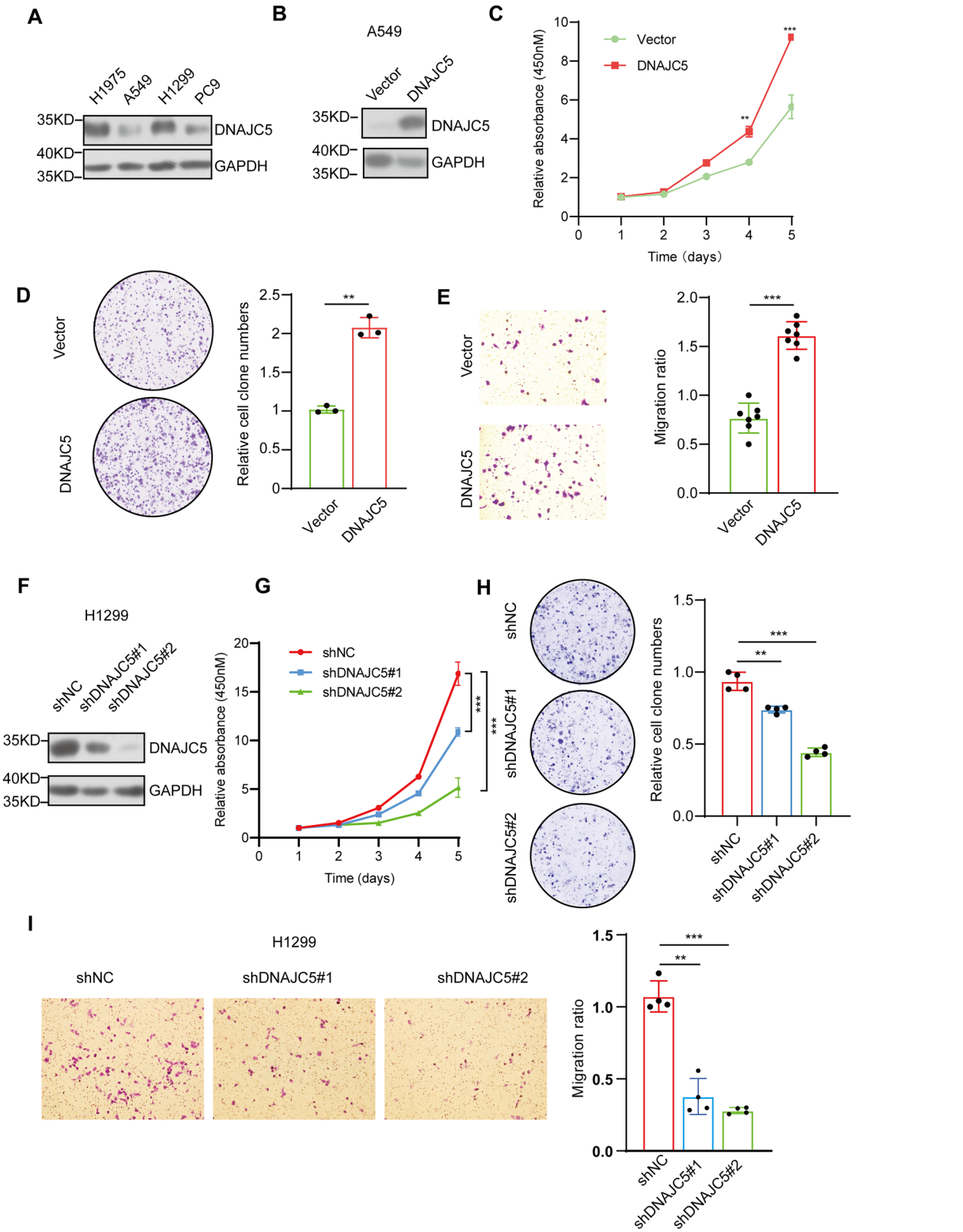

Fig. 2 | DNAJC5 enhances proliferation and migration of LUAD cells. A Protein levels of DNAJC5 were analyzed in four different LUAD cell lines using Western blot analysis. **B** Western blot analysis was performed to assess the protein levels of DNAJC5 in the stable DNAJC5-overexpressing A549 cell line. **C** Cell viability assays using CCK8 showed increased proliferation as indicated (right). **D** Colony formation assays demonstrated enhanced colony formation, as shown. **E** Trans-well assays were conducted to evaluate cell migration rates (left), and the results were quantified (right). **F–I** Knockdown of DNAJC5 suppressed H1299 cell proliferation. **F** Interference efficiency of DNAJC5 was confirmed by Western blot analysis. **G** Cell viability assays using CCK8 revealed decreased proliferation as indicated. **H** The results of colony formation assay demonstrated reduced colony formation. **I** Trans-well assays were performed to assess cell migration rates (left), and the results were quantified (right).

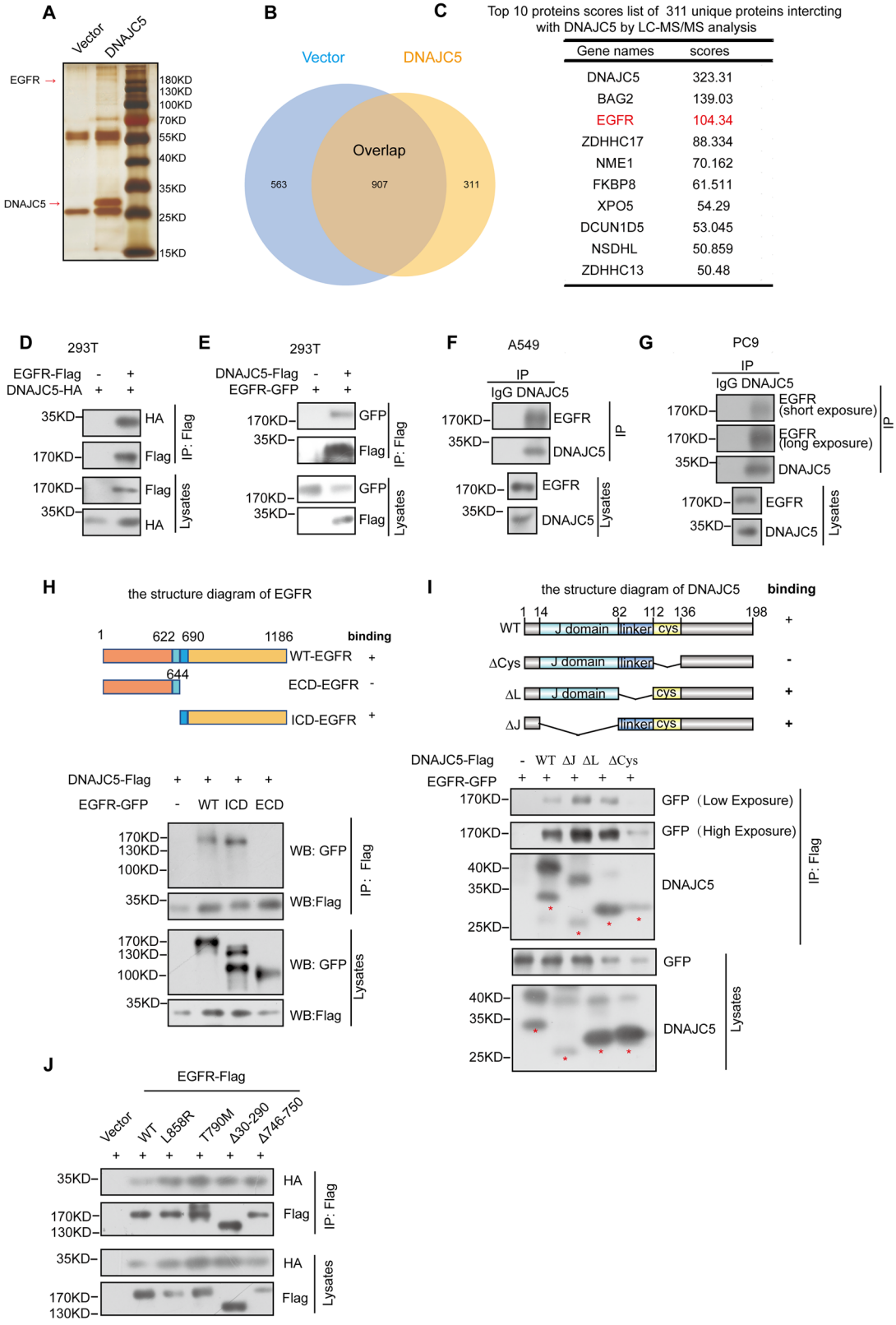

For LC-MS/MS analysis, the bound proteins were extracted from IP beads using SDT lysis buffer (4% SDS, 100 mM DTT, 100 mM Tris-HCl pH 8.0). The IP beads sample was boiled for 3 min and further ultrasonicated. Undissolved beads were removed by centrifugation at 16,000 g for 15 min. The supernatant containing proteins was collected. Protein digestion was performed with the FASP method described by Wisniewski, Zougman et al.[20]. Briefly, the detergent, DTT and IAA in UA buffer were added to block reduced cysteine. Finally, the protein suspension was digested with 2 ug trypsin (Promega) overnight at 37 °C. The peptides were collected by centrifugation at 16,000 g for 15 min. The peptide was desalted with C18 StageTip for further LC-MS analysis. LC-MS/MS experiments were conducted on a Q Exactive HF-X mass spectrometer that was coupled to Easy

Fig. 3 | DNAJC5 interacts with EGFR. A Silver staining was conducted to exhibit DNAJC5 interacted proteins for Mass spectrum analysis. **B** The results of the LC-MS/MS analysis for the identification of potential specific DNAJC5-binding proteins were presented in the Venn diagram. **C** The list of the potential unique proteins with high scores that interacted with DNAJC5 via LC-MS/MS analysis. **D**, **E** The indicated plasmids expressed exogenous EGFR and DNAJC5 were co-transfected into HEK293T cells, and cell lysates were immunoprecipitated and subjected to western blot. **F**, **G** Lysates from A549 cells and PC9 cells were pulled down with anti-DNAJC5 followed by western blot. **H** The domains of EGFR responsible for the DNAJC5 interaction with EGFR were mapped. Schematic illustration of the domains of EGFR (up). Lysates from HEK293T cells co-transfected with the indicated plasmids were incubated with an anti-Flag antibody. The immunoprecipitate (IP) and lysates were probed with the indicated antibodies (down). **I** The domains of DNAJC5 binding EGFR were mapped. Schematic illustration of the domains of DNAJC5 (up). Lysates from HEK293T cells co-transfected with the indicated plasmids were immunoprecipitated and subjected to western blot (down). **J** The indicated plasmids expressed exogenous EGFR mutants and DNAJC5 were co-transfected into HEK293T cells, and cell lysates were immunoprecipitated and subjected to western blot.

nLC1200 (Thermo Scientific) and The MS data were analyzed using MaxQuant software version 1.6.1.0.

Immunofluorescence staining

The lung adenocarcinoma cells were cultured in 24-well plates with round coverslips and subjected to overnight serum starvation. Following stimulation with EGF (10 ng/ml, 236-EG, R&D systems) for the indicated times, the cells were fixed with 4% paraformaldehyde for 15 minutes and permeabilized using 0.5% Triton X-100. Subsequently, the cells were blocked with 2% bovine serum albumin and incubated with primary antibodies at 4 °C. Afterward, fluorochrome-conjugated secondary antibodies and DAPI were applied to the cells for a duration of one hour before observation under a confocal microscope (Leica, Stellaris 5). To assess the co-localization of EGFR and early endosomes marker-EEA1, Leica's LAS X software was employed for signal co-localization analysis.

EGFR endocytosis and recycle assay

Measurements of internalization has been described previously[21]. The cells were washed with ice-cold PBS, followed by biotinylation on ice using 0.5 mg/mL of Sulfo-NHS-SS-biotin (Thermo Scientific, 21331) in PBS (pH= 8.0) and 20 mM HEPES for 40 min at 4 °C. Subsequently, the cells were washed twice with PBS and treated with 100 mM glycine to remove excess biotin before being incubated with DMEM containing EGF for the specified duration. The cell lysates were prepared by washing the cells with ice-cold PBS and lysing them in TNE buffer supplemented with protease inhibitors. Streptavidin Magnetic Beads (MCE, HY-K0208) were utilized overnight to isolate the biotinylated proteins from the cell lysates, followed by western blot analysis.

For recycle assay, after endocytosis, the cells underwent further incubation at 37 °C with EGF (10 ng/ml) for an additional period of either 30 min or 60 min to induce EGFR recycling. Subsequently, the cells were again washed with ice-cold PBS and subjected to cleavage of surface-bound biotin by incubating at 4 °C for 20 min in a solution containing MesNa (10 mM), using as low a concentration as possible.

Cell proliferation and trans-well assay

The proliferative ability of lung adenocarcinoma cells was assessed using clone formation assays and CCK8 assays. For the clone formation assays, lung adenocarcinoma cells were seeded in 6-well plates at a density of 4000 cells/well and cultured for approximately 12 days with regular medium replacement every 2–3 days. The cells were fixed in 4% paraformaldehyde and stained with 0.5% (w/v) crystal violet. Colony quantification was performed using ImageJ software after scanning.

The CCK8 assays were performed in accordance with the manufacturer's instructions. Briefly, CCK8 reagents (Meilunbio, China) were diluted 1:10 with culture medium and added to cells seeded in 96-well plates. After a two-hour incubation period, absorbances were measured at a wavelength of 450 nm using a multimode microplate reader (ThermoFisher, USA).

Transwell assays were employed to assess migratory ability. Transwells with 8.0 μm pore polycarbonate membrane inserts (Corning, USA) were placed in 24-well plates containing medium supplemented with 10% FBS. Subsequently, 30,000 cells were seeded into the transwells using serum-free medium. Following a 48 h incubation period, the cells inside the transwells were gently removed while those outside the transwells were fixed in 4% paraformaldehyde and stained with a solution of 0.5% (w/v) crystal violet. Quantification of cell migration was performed using ImageJ software after scanning.

In vivo xenograft experiment

For the subcutaneous xenograft assay, 1×10^7 A549 cells stably expressing DNAJC5 or control cells were resuspended in sterile PBS (200 μL) and injected subcutaneously into the flanks of 4-week-old female BALB/c-nu athymic nude mice (GemPharmatech Co., Ltd, Nanjing, China). Tumor sizes were recorded every 3 days using Vernier calipers 7 days after injection. Tumor volume was calculated as follows: tumor volume (mm^3) = (length × $width^2$)/2. The mice were sacrificed under anesthesia 28 days after injection, and the tumors were collected for western blotting and immunohistochemistry. Similarly, 2×10^7 H1299 cells stably knocking down DNAJC5 or control cells were injected to BALB/c-nu athymic nude mice and subjected same operation. The protocols for animal experiments were approved by the Ethical Committee of the First Affiliated Hospital of Nanchang University and conformed to the guidelines of the National Institutes of Health on the Ethical Use of Animals. All surgeries were performed after anesthesia and with efforts to minimize suffering.

Hematoxylin-eosin staining and Immunohistochemistry

For hematoxylin and eosin staining, the deparaffinized sections were incubated with hematoxylin for 5 min to stain the nuclei. They were then differentiated with 0.3% acid alcohol for 1 s, incubated with saturated lithium carbonate for 2 s, and finally stained with eosin. The hematoxylin-eosin staining solutions used in this study were obtained from Yulu Experimental Company (Nanchang, China).

Immunohistochemical (IHC) staining was shown as described previously[22]. Briefly, paraffin sections of lung adenocarcinoma tissues and adjacent normal tissues fixed in formalin were mounted on glass slides, deparaffinized, rehydrated, and treated with 3% H2O2 for 10 minutes to block endogenous peroxidase activity. Antigen retrieval was achieved by microwaving the tissues in EDTA buffer (pH 9.0) for 45 minutes followed by overnight incubation at 4 °C with primary antibodies in a humidified chamber. Subsequently, the slides were rinsed with PBS and incubated at 37 °C for 30 min with appropriate biotinylated immunoglobulins (Zhongshan Biotechnology, Zhongshan, China). Immunoreactivity was visualized using the Polink-2 Horseradish Peroxidase DAB Detection kit (Zhongshan Biotechnology) according to the manufacturer's protocol. The samples were independently evaluated and scored by two qualified pathologists using The German semi-quantitative scoring system. The final scores ranged from 0 to12 and represented the expression of DNAJC5. To assess the survival analyses and the correlation between DNAJC5 expression and clinicopathological features, the patients were categorized into two groups based on their immunohistochemistry scores in comparison with the median value. Specifically, those with scores ranging from 0 to 6 were regarded as 'low Expression', and those with scores ranging from 6 to 12 were considered as 'high Expression'.

Clinical tissue samples

In our experiments, the clinical tissue samples were acquired from patients who were diagnosed with lung adenocarcinoma and underwent surgical

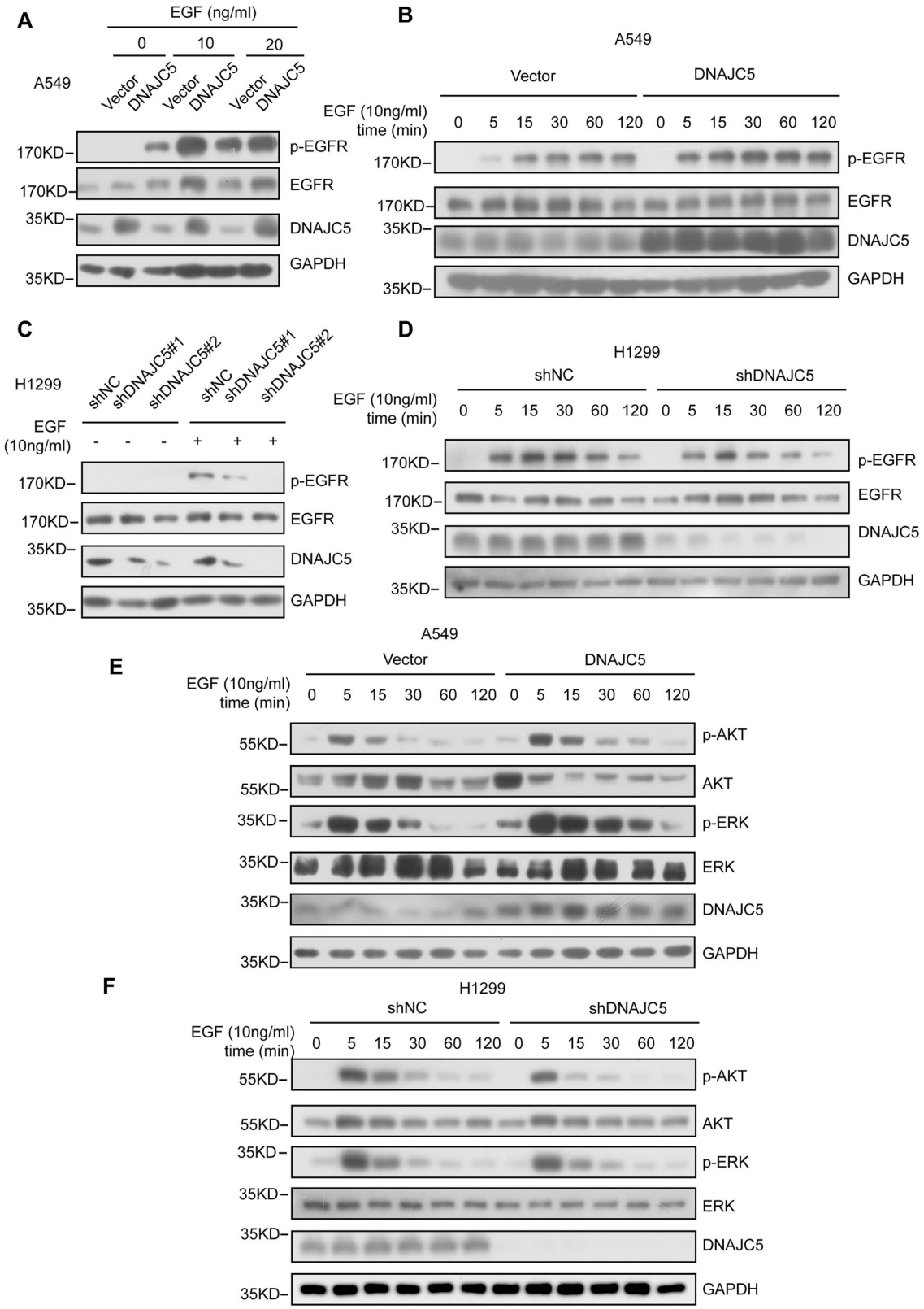

resection at the First Affiliated Hospital of Nanchang University. The clinical tissues including tumors and adjacent normal tissue were examined by a pathologist. This work was approved by the Ethics Committee of the First Affiliated Hospital of Nanchang University (Nanchang, China) [No. (2023) CDYFYYLK (11-005)].

Statistical analysis

The statistical significance of all results was assessed using Student's t-test, one-way analysis of variance (ANOVA), or Mann-Whitney U test. The presented data are representative of at least three independent experiments.

Fig. 4 | DNAJC5 enhances the activity of EGFR and downstream signaling pathways. A A549 cells overexpressing DNAJC5 and control cells were subjected to overnight serum starvation and then treated with varying concentrations of EGF for 15 minutes. The protein levels of EGFR and phosphorylated EGFR (Tyr1068) were analyzed using western blotting. **B** A549 cells overexpressing DNAJC5 and control cells were subjected to overnight serum starvation followed by treatment with EGF (10 ng/ml) for different durations. **C** H1299 cells with knockdown of DNAJC5 expression and control cells were subjected to overnight serum starvation, followed by treatment with EGF (10 ng/ml) for 15 minutes. The protein levels of EGFR and phosphorylated EGFR (Tyr1068) were analyzed using western blotting. **D** H1299 cells with knockdown of DNAJC5 expression and control cells were subjected to overnight serum starvation, followed by treatment with EGF (10 ng/ml) for different durations. **E**, **F** DNAJC5 strengthens AKT and ERK signaling pathways. Cells overexpressing DNAJC5 (**E**), or those in which DNAJC5 was interfered with (**F**), underwent overnight serum starvation before being treated with EGF (10 ng/ml) for different durations. The protein levels of AKT, phosphorylated AKT, ERK, and phosphorylated ERK were analyzed using western blotting.

Reporting summary

Further information on research design is available in the Nature Portfolio Reporting Summary linked to this article.

Results

Elevated DNAJC5 levels are indicators of poor survival for patients with LUAD

The expression levels of DNAJC5 were assessed in LUAD tissues to investigate its role in LUAD progression. Western blot analysis revealed a significantly higher expression of DNAJC5 in tumor samples compared to matched adjacent normal tissues (Fig. 1A). Immunohistochemistry further confirmed these findings (Fig. 1B). Analysis of 232 pairs of LUAD samples demonstrated a significant upregulation of DNAJC5 expression in tumor tissues compared to adjacent normal tissues (Fig. 1C and Figure S1). Survival analyses indicated that increased levels of DNAJC5 were associated with poor overall survival and disease-free survival outcomes for patients (Fig. 1D, E).

Additionally, the correlation between DNAJC5 expression and clinicopathological features was examined by dividing patients into high and low DNAJC5 expression groups based on mean immunohistochemistry scores. The results revealed a positive association between high DNAJC5 expression and poor differentiation ($p = 0.007$, Chi-square test), as well as tumor metastasis ($p = 0.015$, Chi-square test) (Table 1), while no correlations were observed with gender, age, tumor sizes, lymph node metastasis, TNM stage and smoke. Overall, our findings demonstrate the elevated expression of DNAJC5 in LUAD tissues and its association with poor prognosis, suggesting its potential as a prognostic biomarker in LUAD tumorigenesis.

DNAJC5 promotes LUAD cell proliferation and migration

Considering the high expression of DNAJC5 in LUAD tissues, we investigated its function in LUAD cells. Firstly, we established a stable A549 cell line overexpressing DNAJC5, which initially had relatively low levels of DNAJC5 protein (Fig. 2A and Figure S2.A). The protein levels were subsequently detected by Western blot analysis (Fig. 2B). Our results from CCK8 assays and colony formation assays demonstrated that DNAJC5 overexpression significantly promoted the proliferation of A549 cells (Fig. 2C, D). In addition, Table 1 revealed a correlation between DNAJC5 expression and tumor metastasis, prompting us to investigate whether DNAJC5 influenced cell migration. Consistently, our trans-well assay showed that DNAJC5 overexpression increased the migration rate of A549 cells (Fig. 2E). Furthermore, we employed a lentivirus system to knock down DNAJC5 in H1299 cells and confirmed the efficiency of interference through quantitative RT-PCR and Western blot analysis (Figure S2. B and Fig. 2. F). As depicted in Fig. 2G–I. knockdown of DNAJC5 markedly inhibited both cell proliferation and migration. Collectively, these findings provide evidence supporting the role of DNAJC5 as a novel oncogene facilitating non-small lung cancer cell proliferation and migration specifically in LUAD.

DNAJC5 interacts with EGFR

A reported study using affinity purification-mass spectrometry (AP-MS) and proximity-dependent biotinylation (BioID) characterizing the interactome of DNAJC5 found that EGFR might be an interacted partner[23]. Given the irreplaceable role of EGFR in LUAD, we authenticated whether DNAJC5 could bind EGFR. We used SDS-PAGE to separate bound proteins of DNAJC5, which were subsequently silver-stained and analyzed using LC-MS/MS. The result of silver staining showed obvious band of DNAJC5 and a lighter band in 180KD which is the molecular weight of EGFR (Fig. 3A). Subsequent MS analysis identified 311 proteins that specifically interacted with DNAJC5, as depicted in the Venn diagram (Fig. 3B). Among these MS findings, EGFR was included with a high protein score, which was consistent with the previous study (Fig. 3C). Further, The Co-IP assays confirmed exogenous DNAJC5 indeed interacted with EGFR in HEK293T cells (Fig. 3D, E). Similarly, endogenous DNAJC5-EGFR interaction was confirmed in non-small lung cells as well (Fig. 3F, G). Therefore, it is hypothesized that DNAJC5 promotes LUAD cell proliferation and migration by binding to EGFR. Deletion mutants were generated to identify the specific domain on EGFR that interacts with DNAJC5, and results showed that when the "cys-string domain" (Cys) of DNAJC5 was missing, its ability to bind to EGFR was lost, indicating that this region is essential for maintaining the DNAJC5-EGFR interaction (Fig. 3H). Furthermore, it was found that the intracellular domain of EGFR is both necessary and sufficient for interacting with DNAJC5(Fig. 3I). Interestingly, several EGFR mutants including L858R, T790M, Δ30-290 and Δ746-750 also exhibited binding capability towards DNAJC5 (Fig. 3J), suggesting that it may potentially influence the signalling pathway mediated by EGFR.

DNAJC5 enhances EGFR signalling activity

To confirm the hypothesis, we assessed the expression levels of p-EGFR following EGF stimulation in A549 cells overexpressing DNAJC5 or H1299 cells with DNAJC5 knockdown. The results demonstrated that DNAJC5 significantly increased EGFR phosphorylation levels, while knockdown of DNAJC5 decreased p-EGFR levels (Fig. 4A, C). Furthermore, time-course assays of EGF stimulation revealed that DNAJC5 enhanced EGFR phosphorylation at 5 min and sustained it up to 120 min (Fig. 4B). In contrast, p-EGFR levels were reduced at each time point in H1299 cells with DNAJC5 knockdown (Fig. 4D).

The activation of EGFR signaling initiates downstream pathways such as Ras/RAF/MEK, PI3K/AKT/mTOR, and others. We examined the phosphorylation levels of AKT and ERK at different time points (Fig. 4E, F). The results indicated that EGF stimulation induced a rapid peak in p-AKT and p-ERK levels at 5 minutes followed by a gradual decline. Overexpression or knockdown of DNAJC5 modulated the levels of p-AKT and p-ERK at 5 min. Notably, overexpression DNAJC5 dampened while knockdown DNAJC5 accelerated the decay phase of these proteins. These findings demonstrate that DNAJC5 enhances EGFR signaling activity and prolongs downstream signaling.

DNAJC5 promotes EGFR endocytosis and recycle

After activation of EGFR, downstream cascades are initiated, leading to the internalization of EGFR into early endosomes. Subsequently, EGFR is either recycled back to the membrane or transported to lysosomes, which exert feedback control over EGFR signaling. While CME primarily mediates the internalization and recycling of EGFRs back to the plasma membrane at low EGF doses, NCE predominantly directs EGFR trafficking towards lysosomal degradation, resulting in signal extinction[7]. Therefore, we investigated whether DNAJC5 influences EGFR trafficking. A549 cells overexpressing DNAJC5 and control cells were serum-starved overnight and stimulated with EGF (10 ng/ml) for 5 minutes before immunofluorescent staining was

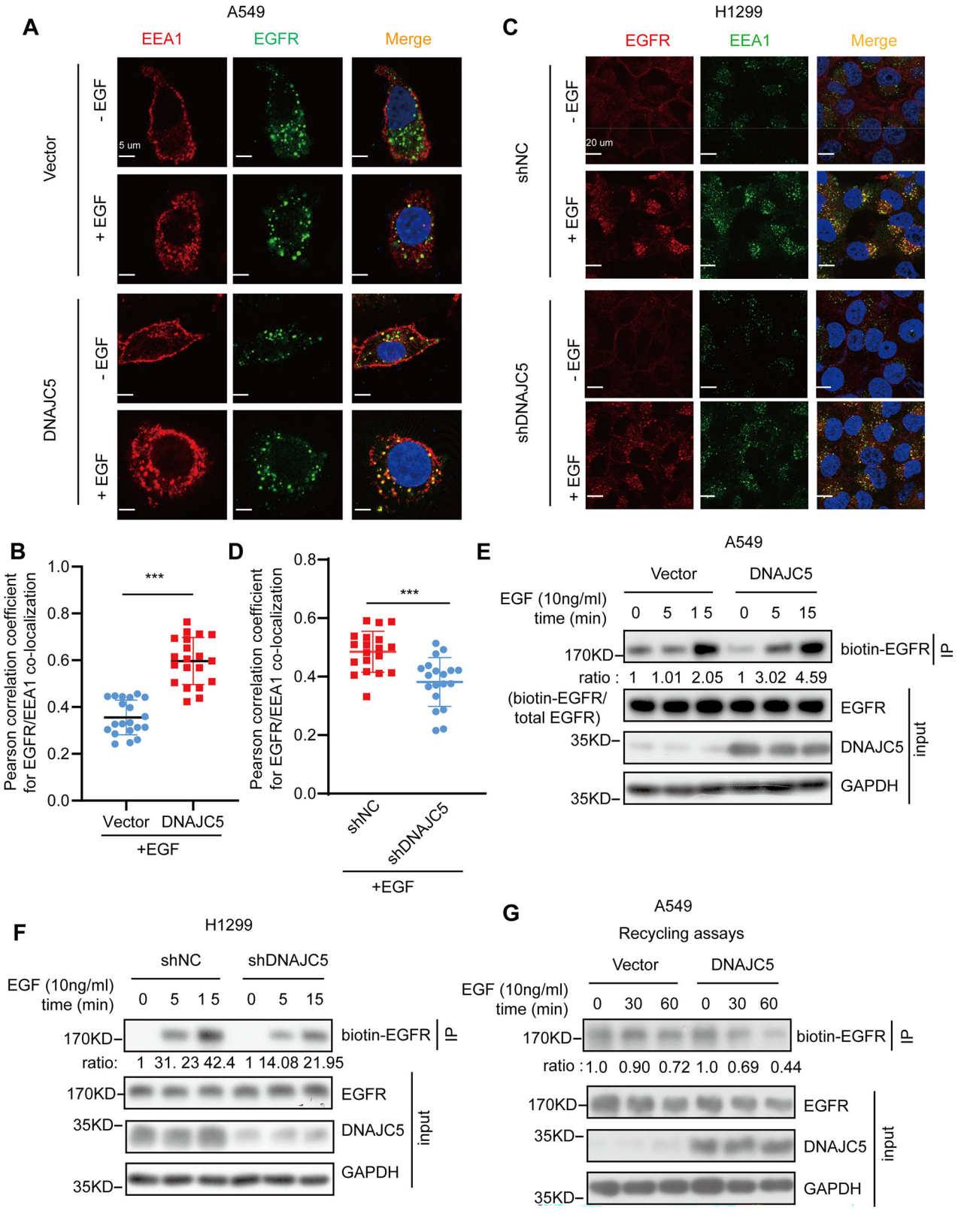

performed. The results demonstrated a significant increase in co-localization between EGFR and the early endosome marker EEA1 (Fig. 5A, B). In contrast, knockdown of DNAJC5 suppressed the internalization of EGFR into early endosomes (Fig. 5C, D). Furthermore, a cell-surface biotinylation assay confirmed that DNAJC5 overexpression enhanced cytoplasmic localization of labeled-EGFR while interference with DNAJC5 had an opposite effect (Fig. 5E, F). Next, we investigated the directionality of EGFR after endocytosis and found that DNAJC5 overexpression also promoted its recycling (Fig. 5G). Collectively, these findings suggest that DNAJC5 facilitates the internalization of EGFR into early endosomes and promotes its recycling back to the plasma membrane potentially enhancing EGFR signal activation.

Fig. 5 | DNAJC5 enhances the endocytosis and recycle of EGFR. **A** Immunofluorescence analysis was performed on serum-starved overnight A549 cells overexpressing DNAJC5 or control A549 cells, with or without treatment with EGF (10 ng/ml) for 15 minutes. Co-localization of EGFR and EEA1 was examined. **B** The degree of colocalization between EGFR and EEA1 was quantified using Pearson's coefficient. **C** Immunofluorescence analysis was conducted on serum-starved overnight H1299 cells with knockdown of DNAJC5 or control cells, with or without treatment with EGF (10 ng/ml) for 15 minutes. Co-localization of EGFR and EEA1 was examined. **D** The degree of colocalization between EGFR and EEA1 was quantified using Pearson's coefficient. **E**, **F** Overexpression of DNAJC5 promoted the endocytosis of EGFR, while knockdown of DNAJC5 suppressed it. To assess internalized EGFR levels, Sulfo-NHS-SS-biotin labeling was performed on ice followed by stimulation with EGF at 37°C for various durations. Cell lysates were immunoprecipitated and subjected to western blotting. Image J software was used to analyze the gray value corresponding to internalized EGFR. **G** Overexpression of DNAJC5 facilitated the recycling process of EGFR. In A549 cells, Sulfo-NHS-SS-biotin labeling on ice followed by stimulation with EGF at 37 °C for 15 minutes allowed surface biotin cleavage by MesNa. Subsequent incubation with EGF at 37 °C for different time periods induced the recycling process in which internalized EGFR returned to the cell surface. Cell lysates were immunoprecipitated and subjected to western blotting. Image J software was used to analyze the gray value corresponding to internalized EGFR.

DNAJC5 enhances the interaction between EGFR and AP2 protein

The clathrin-mediated endocytosis is primarily regulated by clathrin, adaptor protein 2 (AP2), and the large GTPase dynamin[24]. We investigated whether DNAJC5 influences EGFR endocytosis through these proteins. Co-immunoprecipitation results confirmed that DNAJC5 interacts with AP2 complex members (AP2A1, AP2M1, and AP2S1) (Fig. 6A–D). Additionally, DNAJC5 enhanced the interaction between EGFR and AP2A1. Given that EGFR is recognized by AP2 protein, which bridges the cargo to clathrin and drives its internalization via clathrin-coated pits[9], the enhanced binding of EGFR to AP2A1 by DNAJC5 potentially facilitated more EGFR protein into clathrin-coated pits and promoted EGFR endocytosis (Fig. 6E).

If DNAJC5 promotes LUAD cells proliferation and migration depending on EGFR endocytosis, interfering with AP2 expression would attenuate the ability of DNAJC5. As expected, knockdown AP2A1 in DNAJC5-overexpression A549 cells obviously suppressed the cell viability, clonal formation ability and migrated rate (Fig. 6F–K). These results suggested that DNAJC5 promoted LUAD cells proliferation and migration depended on AP2 proteins.

DNAJC5 accelerates LUAD carcinogenesis in vivo

To investigate the impact of DNAJC5 on LUAD in vivo, we established a xenograft mouse model of LUAD tumors using a subcutaneous injection route for tumor cell implantation. Stable A549 cells overexpressing DNAJC5 and control cells were subcutaneously implanted into nude mice flanks. Western blot analysis revealed significantly higher expression levels of DNAJC5 in the xenograft tumor tissues with DNAJC5 overexpression compared to the control group (Fig. 7B). Consistently, the DNAJC5-overexpressing group exhibited notably increased tumor sizes and weights (Fig. 7A–D). Immunohistochemistry results further demonstrated that DNAJC5 upregulated the expression levels of Ki67 and PCNA, which are well-established markers for cell proliferation (Fig. 7E, F). Further, to evaluate the effect of DNAJC5 knockdown on tumorigenesis in vivo, we also established a xenograft model by subcutaneously injecting stable H1299 cells with DNAJC5 knockdown and control cells into the flanks of nude mice. The experimental results demonstrated that DNAJC5 knockdown significantly inhibited tumor growth. Among the eight mice implanted with DNAJC5-knockdown cells, only two developed small tumors, while no detectable tumors were observed in the remaining six mice (Figure S3). These findings provide compelling evidence supporting the role of DNAJC5 in promoting tumor progression in our LUAD xenograft mouse model.

Discussion

Despite recent advancements in surgery, chemotherapy, and targeted molecular therapies, the prognosis for LUAD remains poor, making it imperative to identify new biomarkers and potential therapeutic targets[25]. We discovered that DNAJC5 functions as a novel oncogene in LUAD by significantly promoting cell proliferation and migration. Previous studies have shown that DNAJC5 knockout mice exhibit increased production of neural intermediate progenitor cells due to RGL stem cells losing quiescence and entering a high-proliferation regime. Additionally, interference with DNAJC5 has been found to decrease cell viability in the murine embryonic normal hepatic cell line BNL cl.2, indicating that the effects of DNAJC5 on cell fate are dependent on the specific cell type[15,26]. However, little is known about the role of DNAJC5 in cancer cells until our discovery that it promotes liver cancer cell proliferation and regulates the cell cycle[19]. To further investigate its role in cancer progression, we examined the expression of DNAJC5 in LUAD tissues using immunohistochemistry (IHC) and Western blotting (WB). Our results demonstrated high expression levels of DNAJC5 in LUAD tissues (Fig. 1A–D), with analysis of IHC data revealing a positive correlation between high DNAJC5 expression levels and poor overall survival, disease-free survival, poor differentiation, and tumor metastasis (Fig. 1E, F and Table 1). Consistently, overexpression of DNAJC5 significantly enhanced LUAD cell proliferation and migration (Fig. 2). Furthermore, our findings were validated using an LUAD tumor xenograft mouse model where elevated levels of DNAJC5 promoted tumor growth (Fig. 7). These findings strongly suggest that DNAJC5 plays a crucial role in LUAD progression. however additional research utilizing primary LUAD models is necessary to support this conclusion. The similar results were verified in other members of "DNAJC" family. DNAJC24 and DNAJC12 were reported that could promote lung cancer cells proliferation[27,28]. Interestingly, contrasting effects on LUAD cell proliferation have been observed with two other members of the "J domain" family - DNAJB4 and DNAJA3[29–31]. These results suggest that the impact of "J domain" proteins on LUAD progression is not solely dependent on the conserved "J domain," which activates ATPase activity of HSP70 proteins, but rather involves different targets[27,28].

Indeed, we observed that DNAJC5 interacted with EGFR through exogenous and endogenous co-immunoprecipitation (co-IP), playing a crucial role in driving the progression of LUAD (Fig. 3A–G). Furthermore, DNAJC5 was also capable of binding not only to wild-type but also mutant EGFRs (19del, L858R, T790M) in LUAD cells (Fig. 3J), suggesting its involvement in both types of EGFR-driven LUAD. The deletion of the "cys-string domain" abolished its binding ability, highlighting the significance of this key structural element for DNAJC5's interaction with EGFR (Fig. 3I). Notably, palmitoylation enables the cys-string domain to target lipid membranes like synaptic vesicles and function as a chaperone regulating synaptic vesicle exocytosis[32]. Two mutations in DNAJC5, namely L115R substitution and ΔL116 deletion, disrupt palmitoylation and membrane targeting leading to ANCL development[33]. Investigating the impact of DNAJC5 palmitoylation on LUAD will be addressed in our future studies.

In addition to its role in regulating vesicle exocytosis, DNAJC5 has also been reported to contribute to synaptic vesicle endocytosis by binding with dynamin 1 protein[34]. In motor neurons, DNAJC5 was required for synaptic vesicle recycling and maintenance of synaptic release sites[35]. In our study, we observed the involvement of DNAJC5 in EGFR endocytosis. Upon stimulation with a relatively low dose of EGF (10 ng/ml), DNAJC5 promoted the colocalization between EGFR and the early endosome marker EEA1, while knockdown of DNAJC5 resulted in opposite effects (Fig. 5A–D). Furthermore, a biotin-labeled assay confirmed that DNAJC5 enhanced EGFR endocytosis (Fig. 5E, F). Additionally, we found that DNAJC5 facilitated the recycling process of EGFR back to the plasma membrane (Fig. 5G). Although traditionally considered as weakening EGFR signaling due to its decline on the cell surface, recent studies have demonstrated that endocytosis, especially clathrin-mediated endocytosis (CME), is crucial for sustained EGFR signaling[10,36,37]. At low concentrations of EGF, CME primarily

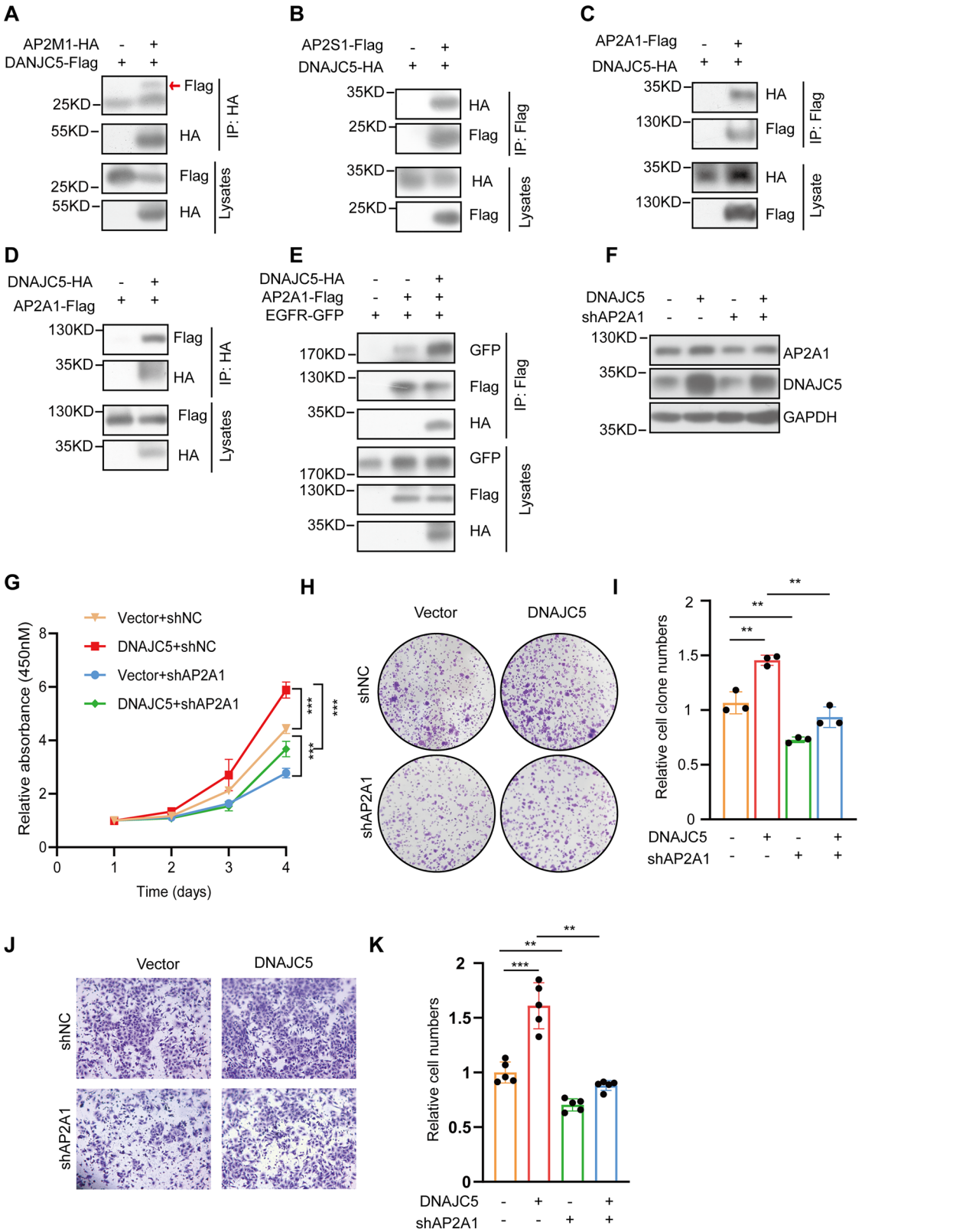

Fig. 6 | DNAJC5 enhances the interaction between EGFR and AP2, thereby promoting proliferation and migration of LUAD cells in an AP2A1-dependent manner. A–D DNAJC5 interacts with various components of the AP2 complex. Plasmids expressing exogenous AP2M1 (**A**), AP2S1 (**B**), or AP2A1 (**C**, **D**) were co-transfected with plasmids expressing DNAJC5 into HEK293T cells. The cell lysates were then immunoprecipitated and subjected to western blot analysis. **E** DNAJC5 strengthens the binding of EGFR to AP2A1. Lysates from cells co-transfected with indicated plasmids were immunoprecipitated and analyzed by western blotting. **F–K** Knockdown DNAJC5 attenuated the ability of DNAJC5 promoting LUAD cell proliferation and migration. **F** AP2A1 was interfered in DNAJC5-overexpressed A549 cells and protein levels was detected by western blot. **G** CCK8 cell viability assays are presented as indicated. **H**, **I** Colony formation assays are shown as indicated and the results were quantified. **J**, **K** Cell migration rates were detected by Trans-well assays, and the results were quantified.

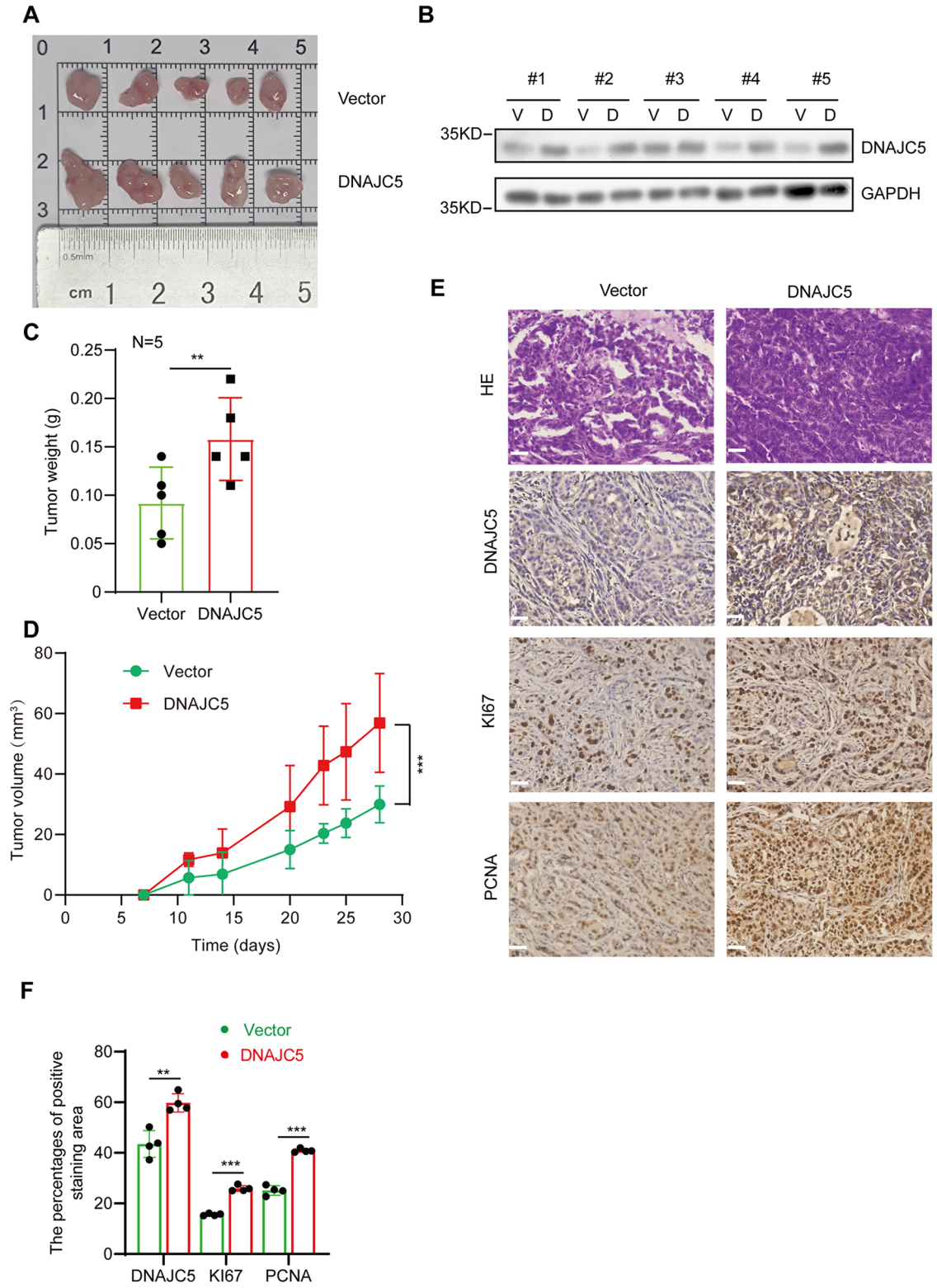

Fig. 7 | DNAJC5 facilitated LUAD carcinogenesis in vivo. Nude mice were subcutaneously injected with $1*10^7$ A549 cells overexpressing DNAJC5 and control cells. **A** The tumors in nude mice are depicted. **B** Western blot analysis confirmed the protein levels of DNAJC5 in xenografts. **C** Tumor weight was quantified in nude mice ($n = 5$). **D** Tumor size was measured at indicated time points, and a tumor growth curve was plotted. **E**, **F** Representative images of immunohistochemistry staining showing DNAJC5, Ki67, and PCNA in subcutaneous tumor models and their quantitative analysis with Image J software.

internalizes and recycles approximately 70% of EGFRs back to the plasma membrane while targeting around 30% for degradation. However, at high concentrations of EGF (20–100 ng/ml), non-clathrin-mediated endocytosis becomes predominant due to saturation of CME pathway. The receptors entering via non-clathrin-mediated pathway (~40%) are mainly directed towards lysosomal degradation leading to signal termination[8]. Our findings demonstrate that DNAJC5 increases phosphorylation levels of EGFR and enhances activity downstream AKT and ERK signaling pathways (Fig. 4). Notably from Fig. 4B, D results under EGF stimulation showed no significant EGFR degradation over time except at 120 min where minimal

degradation was observed. In EGF-stimulated time course assays, DNAJC5 enhanced phosphorylation levels of EGFR at the 5 min and maintained it up to 120 min. Moreover, overexpression or knockdown DNAJC5 dampened or accelerated the decay phase of p-AKT and p-ERK, proving DNAJC5 sustaining EGFR signaling (Fig. 4E, F). These comprehensive findings suggest that DNAJC5 may facilitate EGFR internalization via CME and subsequent recycling, thereby enhancing EGFR signaling activity. However, further detailed and systematic investigations are required to elucidate the precise mechanism by which DNAJC5 regulates CME.

The clathrin-mediated endocytosis is primarily regulated by clathrin, adaptor protein 2 (AP2), and the large GTPase dynamin. AP2 plays a critical role in the assembly of clathrin-coated pits (CCPs) for EGFR clustering and interacts with both clathrin and EGFR[9,38–40]. We found that DNAJC5 can interact with members of the AP2 complex, including AP2A1, AP2M1, and AP2S1 (Fig. 6A, D). Moreover, DNAJC5 significantly enhances the interaction between EGFR and AP2A1 (Fig. 6E), which may explain how DNAJC5 promotes EGFR endocytosis. When we interfered with AP2A1 expression, the ability of DNAJC5 to promote LUAD cell proliferation and migration was correspondingly attenuated (Fig. 6F–K). These results demonstrate that the function of DNAJC5 in LUAD depends on AP2 proteins. In the classical CME model, AP2 was found to be essential for transferrin receptor internalization; however, there is an ongoing discussion regarding its role in EGF-induced EGFR internalization[6]. Some studies have suggested that AP2 only has a mild effect on EGFR internalization[41,42], while other literature indicates stronger effects of AP2[43,44]. It has been explained that differences in experimental procedures, such as cell incubation at 4°C, can lead to varied effects of AP2 on EGFR endocytosis[43], or alternative adaptors may exist for EGFR internalization apart from the AP2 protein[45]. Interestingly, it has also been reported that knockdown of AP2 significantly reduces EGFR recycling and attenuates the activity of both EGFR and downstream signaling pathways[44,45]. These results partially explain our findings that DNAJC5 promotes EGFR endocytosis and recycling through an AP2-dependent mechanism. However, further investigations are required to elucidate the precise mechanism by which DNAJC5 regulates EGFR endocytosis; for instance, exploring the role of DNAJC5 in assembly clathrin-coated pits dependent on AP2.

In general, we have elucidated the oncogenic role of DNAJC5 in LUAD and uncovered its underlying mechanism. Specifically, DNAJC5 acts as a novel adaptor protein for EGFR, enhancing AP2 binding to EGFR and promoting EGFR endocytosis and recycle to potentiate EGFR signaling. Moreover, DNAJC5 facilitates LUAD cell proliferation, migration, and tumor growth. Notably, elevated expression levels of DNAJC5 were observed in LUAD tissues and positively correlated with poor prognosis. These findings provide new insights into the progression of LUAD and offer innovative diagnostic and therapeutic strategies against this disease.

Data availability

Source data for all graphs can be found in Supplementary Data. Unedited and uncropped western blot images are contained in Supplementary Figure within the Supporting Information. The mass spectrometry proteomics data have been deposited to the Proteome Xchange Consortium via the PRIDE partner repository with the dataset identifier PXD063682. Other requests for source data can be accommodated by the corresponding author upon reasonable request.

Received: 27 June 2024; Accepted: 7 May 2025;
Published online: 15 May 2025

References

1. Siegel, R. L., Miller, K. D., Wagle, N. S. & Jemal, A. Cancer statistics, 2023. *CA Cancer J. Clin.* **73**, 17–48 (2023).
2. Thai, A. A., Solomon, B. J., Sequist, L. V., Gainor, J. F. & Heist, R. S. Lung cancer. *Lancet* **398**, 535–554 (2021).
3. Levantini, E., Maroni, G., Del Re, M. & Tenen, D. G. EGFR signaling pathway as therapeutic target in human cancers. *Semin Cancer Biol.* **85**, 253–275 (2022).
4. Passaro, A., Janne, P. A., Mok, T. & Peters, S. Overcoming therapy resistance in EGFR-mutant lung cancer. *Nat. Cancer* **2**, 377–391 (2021).
5. Shi, K. et al. Emerging strategies to overcome resistance to third-generation EGFR inhibitors. *J. Hematol. Oncol.* **15**, 94 (2022).
6. Tomas, A., Futter, C. E. & Eden, E. R. EGF receptor trafficking: consequences for signaling and cancer. *Trends Cell Biol.* **24**, 26–34 (2014).
7. Sigismund, S., Avanzato, D. & Lanzetti, L. Emerging functions of the EGFR in cancer. *Mol. Oncol.* **12**, 3–20 (2018).
8. Caldieri, G. et al. Reticulon 3-dependent ER-PM contact sites control EGFR nonclathrin endocytosis. *Science* **356**, 617–624 (2017).
9. Caldieri, G., Malabarba, M. G., Di Fiore, P. P. & Sigismund, S. EGFR Trafficking in Physiology and Cancer. *Prog. Mol. Subcell. Biol.* **57**, 235–272 (2018).
10. Kim, B. et al. Clathrin-mediated EGFR endocytosis as a potential therapeutic strategy for overcoming primary resistance of EGFR TKI in wild-type EGFR non-small cell lung cancer. *Cancer Med.* **10**, 372–385 (2021).
11. Jo, U. et al. EGFR endocytosis is a novel therapeutic target in lung cancer with wild-type EGFR. *Oncotarget* **5**, 1265–1278 (2014).
12. Gundersen, C. B. Cysteine string proteins. *Prog. Neurobiol.* **188**, 101758 (2020).
13. Burgoyne, R. D. & Morgan, A. Cysteine string protein (CSP) and its role in preventing neurodegeneration. *Semin Cell Dev. Biol.* **40**, 153–159 (2015).
14. Lopez-Ortega, E., Ruiz, R. & Tabares, L. CSPalpha, a Molecular Co-chaperone Essential for Short and Long-Term Synaptic Maintenance. *Front Neurosci.* **11**, 39 (2017).
15. Nieto-Gonzalez, J. L. et al. Loss of postnatal quiescence of neural stem cells through mTOR activation upon genetic removal of cysteine string protein-alpha. *Proc. Natl Acad. Sci. USA* **116**, 8000–8009 (2019).
16. Noskova, L. et al. Mutations in DNAJC5, encoding cysteine-string protein alpha, cause autosomal-dominant adult-onset neuronal ceroid lipofuscinosis. *Am. J. Hum. Genet* **89**, 241–252 (2011).
17. Roosen, D. A., Blauwendraat, C., Cookson, M. R. & Lewis, P. A. DNAJC proteins and pathways to parkinsonism. *FEBS J.* **286**, 3080–3094 (2019).
18. Donnelier, J. & Braun, J. E. CSPalpha-chaperoning presynaptic proteins. *Front Cell Neurosci.* **8**, 116 (2014).
19. Wang, H. et al. DNAJC5 promotes hepatocellular carcinoma cells proliferation though regulating SKP2 mediated p27 degradation. *Biochim Biophys. Acta Mol. Cell Res.* **1868**, 118994 (2021).
20. Wisniewski, J. R., Zougman, A., Nagaraj, N. & Mann, M. Universal sample preparation method for proteome analysis. *Nat. Methods* **6**, 359–362 (2009).
21. Barral, D. C. et al. CD1a and MHC class I follow a similar endocytic recycling pathway. *Traffic* **9**, 1446–1457 (2008).
22. Wang, Y. et al. The critical role of dysregulated Hh-FOXM1-TPX2 signaling in human hepatocellular carcinoma cell proliferation. *Cell Commun. Signal* **18**, 116 (2020).
23. Piette, B. L. et al. Comprehensive interactome profiling of the human Hsp70 network highlights functional differentiation of J domains. *Mol. Cell* **81**, 2549–2565 e2548 (2021).
24. McMahon, H. T. & Boucrot, E. Molecular mechanism and physiological functions of clathrin-mediated endocytosis. *Nat. Rev. Mol. Cell Biol.* **12**, 517–533 (2011).
25. Singh, T., Fatehi Hassanabad, M. & Fatehi Hassanabad, A. Non-small cell lung cancer: Emerging molecular targeted and immunotherapeutic agents. *Biochim Biophys. Acta Rev. Cancer* **1876**, 188636 (2021).

26. Kang, J. S. et al. Evaluation of Potential Biomarkers for Thioacetamide-induced Hepatotoxicity using siRNA. *Biomolecules Therapeutics* **16**, 197–202 (2008).
27. Li, Y. et al. DNAJC12 promotes lung cancer growth by regulating the activation of β-catenin. *Int. J. Mol. Med.* **47**, 105 (2021).
28. Liu, D. et al. DNAJC24 acts directly with PCNA and promotes malignant progression of LUAD by activating phosphorylation of AKT. *FASEB J.* **38**, e23630 (2024).
29. Tsai, M. F. et al. A new tumor suppressor DnaJ-like heat shock protein, HLJ1, and survival of patients with non-small-cell lung carcinoma. *J. Natl Cancer Inst.* **98**, 825–838 (2006).
30. Wang, C. C. et al. The transcriptional factor YY1 upregulates the novel invasion suppressor HLJ1 expression and inhibits cancer cell invasion. *Oncogene* **24**, 4081–4093 (2005).
31. Chen, C. Y. et al. Tid1-L inhibits EGFR signaling in lung adenocarcinoma by enhancing EGFR Ubiquitinylation and degradation. *Cancer Res.* **73**, 4009–4019 (2013).
32. Wu, S. et al. Unconventional secretion of α-synuclein mediated by palmitoylated DNAJC5 oligomers. *Elife* **12**, e85837 (2023).
33. Greaves, J. et al. Palmitoylation-induced aggregation of cysteine-string protein mutants that cause neuronal ceroid lipofuscinosis. *J. Biol. Chem.* **287**, 37330–37339 (2012).
34. Zhang, Y. Q. et al. Identification of CSPalpha clients reveals a role in dynamin 1 regulation. *Neuron* **74**, 136–150 (2012).
35. Rozas, J. L. et al. Motorneurons require cysteine string protein-alpha to maintain the readily releasable vesicular pool and synaptic vesicle recycling. *Neuron* **74**, 151–165 (2012).
36. Pinilla-Macua, I., Grassart, A., Duvvuri, U., Watkins, S. C., Sorkin, A. EGF receptor signaling, phosphorylation, ubiquitylation and endocytosis in tumors in vivo. *Elife.***6**, e31993 (2017).
37. Sigismund, S. et al. Threshold-controlled ubiquitination of the EGFR directs receptor fate. *EMBO J.* **32**, 2140–2157 (2013).
38. Conte, A. & Sigismund, S. Chapter Six - The Ubiquitin Network in the Control of EGFR Endocytosis and Signaling. *Prog. Mol. Biol. Transl. Sci.* **141**, 225–276 (2016).
39. Goh, L. K., Huang, F., Kim, W., Gygi, S. & Sorkin, A. Multiple mechanisms collectively regulate clathrin-mediated endocytosis of the epidermal growth factor receptor. *J. Cell Biol.* **189**, 871–883 (2010).
40. Collins, B. M., McCoy, A. J., Kent, H. M., Evans, P. R. & Owen, D. J. Molecular architecture and functional model of the endocytic AP2 complex. *Cell* **109**, 523–535 (2002).
41. Motley, A., Bright, N. A., Seaman, M. N. & Robinson, M. S. Clathrin-mediated endocytosis in AP-2-depleted cells. *J. Cell Biol.* **162**, 909–918 (2003).
42. Johannessen, L. E., Pedersen, N. M., Pedersen, K. W., Madshus, I. H. & Stang, E. Activation of the epidermal growth factor (EGF) receptor induces formation of EGF receptor- and Grb2-containing clathrin-coated pits. *Mol. Cell Biol.* **26**, 389–401 (2006).
43. Rappoport, J. Z. & Simon, S. M. Endocytic trafficking of activated EGFR is AP-2 dependent and occurs through preformed clathrin spots. *J. Cell Sci.* **122**, 1301–1305 (2009).
44. Sigismund, S. et al. Clathrin-mediated internalization is essential for sustained EGFR signaling but dispensable for degradation. *Dev. Cell* **15**, 209–219 (2008).
45. Pascolutti, R. et al. Molecularly Distinct Clathrin-Coated Pits Differentially Impact EGFR Fate and Signaling. *Cell Rep.* **27**, 3049–3061 e3046 (2019).

Acknowledgements

This work was supported by grants from National Natural Science Foundation of China (82160507), Natural Science Foundation of Jiangxi Province (No.20232ACB206034 to H.W., No.20232BCJ23013 to L.C., No.20202BBG72003 to S.L.), the National Natural Science Foundation of China (No. 32260160 to M.C., No.32300599 to L.C., No.32070783 to S.L., No.82060517 to X.L.).

Author contributions

Conception and design: Hailong Wang. Acquisition of data: Canchen, Linlin Xu, Hailong Wang. Analysis and interpretation of data: Hailong Wang, Zhenyu Zhai, Canchen. Writing, review and/or revision of the manuscript: Hailong Wang, Limin Chen. Administrative, technical, or material support: Minzhang Cheng, Limin Chen. Study supervision: Shiwen Luo.

Competing interests

The authors declare no competing interests.

Ethics approval and consent to participate

All experiments involving human tissue samples were approved by the Ethics Committee of the First Affiliated Hospital of Nanchang University (Nanchang, China).

Additional information

Supplementary information The online version contains supplementary material available at https://doi.org/10.1038/s42003-025-08191-9.

Correspondence and requests for materials should be addressed to Shiwen Luo or Hailong Wang.

Peer review information *Communications Biology* thanks Hidetoshi Hayashi and the other, anonymous, reviewer for their contribution to the peer review of this work. Primary Handling Editors: Bibekanand Mallick and Mengtan Xing.